J Radioanal Nucl Chem (2017) 311:85–97
DOI 10.1007/s10967-016-5043-7

Sorption separation of cobalt and cadmium by straw-derived biochar: a radiometric study

Martin Pipíška[1,2] · Barbora Micháleková Richveisová[1] · Vladimír Frišták[3] · Miroslav Horník[1] · Lucia Remenárová[1] · Richard Stiller[1] · Gerhard Soja[3]

Received: 14 April 2016 / Published online: 19 September 2016

Abstract Biochar prepared from *Triticum aestivum* straw (SB) was used to investigate the sorption separation of Cd^{2+} and Co^{2+} ions in single and binary systems. The maximum adsorption capacity of SB was higher for Cd^{2+} ions and the process was strongly pH dependent. Adsorption data in the binary system Cd^{2+}–Co^{2+} were well described by the extended Langmuir model and the values of affinity parameter *b* indicate a higher affinity of SB to Cd^{2+} in comparison with Co^{2+} ions. The mechanisms for the removal of Cd and Co by biochar were evidenced by the different instrumental analyses as well as by chemical speciation modeling. Elemental mapping of SB revealed spatial distributions of cobalt and cadmium on biochar surfaces. The role of functional groups in metal sorption was confirmed by FTIR. Results demonstrate that SB is a promising heavy metal-immobilizing agent for contaminated soils or water.

Keywords Straw biochar · ^{60}Co · ^{109}Cd · Adsorption · Binary system · Mechanism

✉ Martin Pipíška
pipiska@ucm.sk; pipiskam@gmail.com

[1] Department of Ecochemistry and Radioecology, Faculty of Natural Sciences, University of SS. Cyril and Methodius in Trnava, J. Herdu 2, 917 01 Trnava, Slovak Republic

[2] Department of Chemistry, Trnava University in Trnava, Priemyselná 4, 918 43 Trnava, Slovak Republic

[3] Energy Department, AIT Austrian Institute of Technology GmbH, Konrad-Lorenz-Straße 24, 3430 Tulln an der Donau, Austria

Introduction

Sorption separation of heavy metals and radionuclides has appeared as a highly competitive method to conventional methods of waste water treatment. Despite high effectivity of ion-exchange, electro-coagulation, precipitation, and membrane separation, currently sorption with application of low-cost materials represents a promising alternative separation technology. Many publications on the topic of sorption separation ([44, 45], Frišták et al. [14]) showed the potential of natural and artificial sorbents to purify large volumes of radioactively contaminated aqueous solutions from nuclear industry and from water bodies or seepage waters of contaminated areas [54]. Additionally, natural sorption materials (zeolites, bentonites) found utilization as engineered barriers to mitigate radionuclide migration in the deep geological repositories of high-level radioactive waste and spent nuclear fuel [1, 17]. Carbon-based sorption materials such as activated carbon, carbon fibers or carbon nanotubes revealed the option to apply thermochemical conversion processes to different input materials, thereby producing sorbents with various properties and sorption characteristics. Recently, biochar as a solid by-product from slow or fast pyrolysis processes established its position in the system of carbon sorption materials and thus opened a new direction in the portfolio of sorbents [15]. Input feedstock and pyrolysis conditions such as temperature (300–700 °C), highest temperature holding time, pressure or presence of chemical agents (catalysts) affect the physicochemical transformation of biomass and its subsequent ability to sorb contaminants. It is important to notice that after the pyrolysis process biochar derived from various feedstocks has a highly porous structure and contains oxygen-containing functional groups, which are most responsible to bind inorganic and organic pollutants on

external but also internal surfaces [58] even from much diluted solutions. A promising field of application for biochar is environmental remediation [2, 15]. Biochar produced from various feedstocks showed high equilibrium sorption capacities for contaminants such as Pb(II), Cd(II) and Zn(II) in modulated in situ batch sorption systems and in contaminated field sites as well [24, 47, 51]. Various mechanisms were described to explain heavy metal sorption to biochar surfaces, such as cation exchange, complexation, electrostatic attraction and cation-π bonding [12, 49]. Cao et al. [7] used dairy-manure derived biochar for remediation of Pb contaminated soil and they found that biochar is effective in Pb sorption with a sorption capacity up to 680 mmol Pb kg^{-1}. Yakkala et al. [61] investigated the sorption of Cd^{2+} and Pb^{2+} by biochar derived from buffalo weed. They found maximum adsorption capacities of 103 and 1609 mmol kg^{-1} for Cd^{2+} and Pb^{2+}, respectively, based on Langmuir equations. Inyang et al. [24] reported about the potential of two biochars produced from anaerobically digested biomass to sorb heavy metals (Pb^{2+}, Cu^{2+}, Ni^{2+} and Cd^{2+}). Comparing the digested dairy waste biochar and digested whole sugar beet biochar, the latter had higher capacity to remove Ni and Cd. There are also many studies on the competitive sorption of heavy metals in multi-metal system using various sorbent such as zeolites (e.g. [46], soils (e.g. [18] and agricultural biomass (e.g. [59], but only few studies have examined the competitive sorption of heavy metals by biochar. Park et al. [41] have reported adsorption behaviour of heavy metals in mono- and multi-metal forms by sesame straw derived biochar. Their results showed that adsorption capacities from the multi-metal adsorption isotherms were in the order of Pb » Cu » Cr > Zn » Cd. This shows the necessity to investigate heavy metal sorption in multi-metal systems in order to specify the fate of these elements in the natural environment.

Considering the above mentioned findings and the fact that a competitive sorption study of cobalt and cadmium by straw-derived biochar has not been reported previously, the key objectives of our research were [1] to describe the Cd^{2+} and Co^{2+} ions binding onto a biochar-based sorbent from single and binary component solutions and [2] to elucidate the mechanisms responsible for metal binding using FTIR, SEM, EDX elemental mapping and chemical speciation modelling. The radioindicator method with radionuclides ^{109}Cd and ^{60}Co were used to obtain precise and reliable characterization of Cd and Co sorption separation in a wide concentration range both in single and binary systems. The potential of straw biochar as a promising toxic metal and radionuclide adsorbent for contaminated soils or water also has been evaluated.

Materials and methods

Sorbent preparation

Triticum aestivum straw has been pyrolysed in a slow pyrolysis process at a highest treatment temperature of 525 °C (residence time 2 h) in a modified lab-scale pyrolysis reactor. Inert and uniform heating conditions were ensured by nitrogen (N_2) as a flush gas. Obtained straw biochar (SB) was washed twice in deionized water with conductivity <0.4 μS cm^{-1} (Simplicity 185, Millipore, USA) in order to remove impurities, oven-dried for 72 h at 90 °C, ground, sieved and the fraction <125 μm was used in metal sorption experiments.

Surface area measurements

For determination of specific surface area and pore size of the SB samples the technique of nitrogen adsorption and desorption was performed using the Sorptomatic 1990 specific surface area analyzer (Thermo Finnigan, Milano, Italy). The obtained data were evaluated by Brunauer-Emmett-Tellers (BET) adsorption model in (0–0.25) p/p_0. The micropore (V_{mi}) and mesopore (V_{me}) volumes were also determined from the isotherm and the distribution of mesopores (pore width 2–50 nm) was evaluated using the BJH model (Barrett-Joyner-Halenda) [5]. For determination of the micropores (pore width 0–2 nm) distribution, the Horvath-Kawazoe model [23] was used.

Adsorption experiments in single system

All solutions of $CdCl_2$ (analytical grade; CAS 10108-64-2; Sigma-Aldrich, USA) and $CoCl_2$ (analytical grade; CAS 7646-79-9; Sigma-Aldrich, USA) were prepared in deionised water. Batch adsorption kinetics experiments were carried out by suspending SB (2.5 g dm^{-3}, d.w.) in cobalt and cadmium solutions (C_0 = 1000 μmol dm^{-3} of $CoCl_2$ spiked with ^{60}Co or 1000 μmol dm^{-3} of $CdCl_2$ spiked with ^{109}Cd at pH adjusted to 6.0) and shaken on a reciprocal shaker (Environmental shaker ES20, Biosan, Latvia) at 120 rpm at 22 °C. During the adsorption process, aliquot samples were taken from individual flasks at 10, 30, 60, 120, 240 and 1440 min and radioactivity was measured using scintillation gamma-spectrometry.

To determine the sorption capacity of SB, batch adsorption experiments were carried out in solutions ranging from 100 to 4000 μmol dm^{-3} of $CdCl_2$ or $CoCl_2$ in deionised water, spiked with $^{109}CdCl_2$ or $^{60}CoCl_2$ and adjusted to pH 6.0. SB (2.5 g dm^{-3} d.w.) was added, and the content was agitated on a reciprocal shaker at 120 rpm

for 4 h at 20 °C. Contact time 4 h was sufficient to reach equilibrium which was shown in preliminary experiments.

To analyze the influence of pH on the sorption of Co and Cd, straw biochar (2.5 g dm^{-3} d.w.) was shaken in Co^{2+} and Cd^{2+} solutions (C_0 = 1000 μmol dm^{-3}) of desired pH (2.0 to 8.0) spiked with $^{60}CoCl_2$ and $^{109}CdCl_2$ for 4 h on a reciprocal shaker at 120 rpm and at 22 °C. In order to eliminate interference of buffer components on sorption, the non-buffered solutions in deionized water were adjusted to the desired pH values by adding 0.5 mol dm^{-3} HCl or 0.1 mol dm^{-3} NaOH.

At the end of each experiment SB samples were centrifuged, filtered and washed twice with deionized water with a conductivity <0.4 μS cm^{-1}. Radioactivity of the liquid and solid phases was measured. All experiments were performed in duplicates. If not stated otherwise, presented data are arithmetic mean values.

The uptake of Co^{2+} and Cd^{2+} ions by straw biochar was calculated as:

$$Q_{eq} = (C_0 - C_{eq})\frac{V}{M} \quad (1)$$

where Q_{eq} is the metal uptake (μmol g^{-1}), C_0 and C_{eq} are the initial and the final metal concentrations in solution (μmol dm^{-3}), V is volume (L) and M is the amount of dried sorbent (g).

Adsorption experiments in binary system

Batch sorption experiments were carried out in binary solutions of Cd^{2+}–Co^{2+} containing each metal in concentrations varying from 100 to 4000 μmol dm^{-3} in various molar ratios 2:1, 1:1, 1:2 spiked with $^{109}CdCl_2$ and $^{60}CoCl_2$. pH was adjusted to 6.0 with 0.1 mol dm^{-3} NaOH. Straw biochar (2.5 g dm^{-3} d.w.) was added, and the content in flasks was agitated on a reciprocal shaker (120 rpm) for 4 h at 22 °C. At the end of each experiment, the SB was filtered out, washed twice with deionized water and the radioactivity of both the SB and the liquid phase was measured. All experiments were performed in duplicates. If not otherwise stated, presented data are arithmetic mean values. The metal uptake of Cd^{2+} and Co^{2+} ions from binary Cd^{2+}–Co^{2+} system was calculated according to Eq. [1].

FTIR and SEM-EDX analysis

The functional groups present on the SB and the Cd and Co loaded SB were determined by FTIR analysis (Nicolet NEXUS 470 spectrometer, Thermo Scientific, USA) using the KBr pellet technique (SB:KBr 1:100). The FTIR spectra were obtained within the range of 4000–400 cm^{-1}. The surface structure analysis of the SB before and after $Co^{2+}$and Cd^{2+} ions sorption from single systems and EDX microanalysis were performed by scanning electron microscope VEGA 2 SEM (TESCAN s.r.o., Czech Republic) coupled with an EDX, QUANTAX QX2 detector (RONTEC, Germany) for electron dispersive X-ray analysis. Prior the SEM and EDX analysis, the samples of SB were dried (60 °C, 72 h) and glued to an aluminium sample holder using conductive adhesive (Ag). Samples were then coated with Au using BP 343.7 Evaporator (TESLA ELMI a.s., Czech Republic). The analyses were performed at voltage 30 kV, vacuum pressure 9.0 × 10^{-3} Pa and magnification 250×.

Radiometric analysis

All solutions used in the experiments were spiked with $^{109}CdCl_2$ (3.857 MBq cm^{-3}; $CdCl_2$ 50 mg dm^{-3} in 3 g dm^{-3} HCl) and $^{60}CoCl_2$ (5.181 MBq cm^{-3}, $CoCl_2$ 20 mg dm^{-3} in 3 g dm^{-3} HCl) solutions obtained from the Czech Metrological Institute (Czech Republic). The radiometric analysis of ^{109}Cd and ^{60}Co in straw biochar samples and supernatant fluids was performed using a well type NaI(Tl) scintillation gamma-spectrometer 54BP54/2-X or 76BP76/3 (Scionix, The Netherlands or Envinet, Czech Republic) and the data processing software ScintiVision-32 (Ortec, USA). For energy and efficiency calibration, a library of radionuclides was built by selecting characteristic γ-ray peaks for ^{109}Cd (E_γ = 88.04 keV) or ^{60}Co (E_γ = 1173.24 keV), and for the calibration, standard solutions of $^{109}CdCl_2$ and $^{60}CoCl_2$ with known radioactivity including the half-life of radionuclides (^{109}Cd: $T_{1/2}$ = 462.6 d and ^{60}Co: $T_{1/2}$ = 1925.4 d) were used.

Speciation modelling

The prediction of Co and Cd speciation in solution as a function of pH, temperature, ionic strength, and concentrations of cations and anions was calculated using the modelling software Visual MINTEQ (version 3.0) program. Visual MINTEQ is a chemical equilibrium program that has an extensive thermodynamic database for the calculation of metal speciation, solubility and equilibria [19]. All data sets were calculated considering the carbonate system naturally in equilibrium with atmospheric CO_2 (pCO_2 = 38.5 Pa).

Data analysis

The adsorption equilibrium data were described by adsorption isotherms according to the Langmuir (Eq. 2; [31] and Freundlich (Eq. 3; [13] equations. The non-linear forms of these mathematical models are as follows:

$$Q_{eq} = \frac{bQ_{\max}C_{eq}}{1 + bC_{eq}} \quad (2)$$

$$Q_{eq} = KC_{eq}^{(1/n)} \quad (3)$$

where C_{eq} is the equilibrium concentration of the metal ions in the solution (mg dm^{-3}), Q_{eq} is the equilibrium specific sorption of metal ions onto the SB (mg g^{-1}; d.w.), Q_{max} is the maximum sorption capacity of the SB(mg g^{-1}; d.w.), b is the Langmuir equilibrium constant characterizing the affinity between the metal ions and the SB (dm^3 mg^{-1}), K is the Freundlich equilibrium constant related to sorption capacity of the SB (dm^3 g^{-1} of SB), n is the Freundlich equilibrium constant related to intensity of the sorption (non-dimensional).

The Q_{max} values and the corresponding parameters of adsorption isotherms were calculated using the non-linear regression analysis performed by ORIGIN 8.0 Professional (OriginLab Corporation, Northampton, USA).

The extended Langmuir model [4, 37] was used for quantitative interpretation of sorption equilibrium in Co-Cd binary system. The expressions of extended Langmuir model are as follows:

$$Q_{eq}[M] = \frac{Q_{\max M}b_M C_{eq}[M]}{1 + b_M C_{eq}[M] + b_N C_{eq}[N]} \quad (4)$$

$$Q_{eq}[N] = \frac{Q_{\max N}b_N C_{eq}[N]}{1 + b_M C_{eq}[M] + b_N C_{eq}[N]} \quad (5)$$

$$b_M = \frac{1}{K_M} \text{ and } b_N = \frac{1}{K_N} \quad (6)$$

where $Q_{eq}[M]$ and $Q_{eq}[N]$ are equilibrium sorption capacities of metals M and N in binary system, $C_{eq}[M]$ and $C_{eq}[N]$ represent equilibrium concentrations of metals remaining in solution and Q_{maxM} and Q_{maxN} are the maximum sorption capacities of individual metals in binary system. The parameters b_M and b_N represent affinity constants of Langmuir model for the first and second metal ions and K_M and K_N equilibrium constants for binding sites occupied with metal M and N, respectively.

The 3D sorption surfaces for binary system Co^{2+}–Cd^{2+} were obtained by plotting the experimental Co^{2+} and Cd^{2+} equilibrium concentrations C_{eq} on the X and Y axes, against the cadmium or cobalt uptake Q_{eq} on the Z axis. The TableCurve 3D 4.0 program (Systat Software, Inc., Chicago, USA) was used for this purpose.

Results and discussion

Biochar characterization

The main physico-chemical properties of the studied straw-derived biochar are given in Table 1 in comparison with different biochars. The total C, H and N content of SB was 74.4, 2.83 and 1.04 % respectively. The differences in elemental composition of straw-derived biochars were found due to feedstocks and pyrolysis conditions, such as temperature and residence time. Higher pyrolysis temperature caused the increase of C content and decrease of total H content resulting in lower molar H/C ratio which indicates dehydration of the input biomass [3]. Comparison of the N content of different straw biochars showed no significant effect of pyrolysis temperature on N content. The C/N molar ratio of biochar ranged from 78 to 180 (Table 1). The N content of biochar is mainly determined by the origin of the feedstocks. Keiluweit et al. [25] described that the positions of plant-derived biochars in the van Krevelen diagram and lower molar H/C and O/C ratios confirm dehydratation and depolymerization of biomass into dissociation products of lignin and cellulose with increasing treating temperatures. This is confirmed also by Liu et al. [34], who described that lignin undergoes dehydratation and depolymerisation during the pyrolysis process.

The surface area of studied SB determined from BET isotherm was 66.79 m^2 g^{-1}, which was significantly higher compared to corn straw biochar and wheat straw produced at 500 °C, but considerably lower compared to wheat straw biochar produced at high pyrolysis temperatures (750 and 700 °C, Table 1). This is consistent with the fact that not only biochar feedstock but also pyrolysis temperature significantly affected the biochar surface area [16]. Chen and Chen [9] reported that the increase in surface area at higher pyrolysis temperatures could be caused by the destruction of aliphatic alkyl and ester groups, and exposure of the aromatic lignin core. Thermal treatment also affects pore volume, which results in a large specific surface area [16]. Total pore volume of SB was 0.206 cm^3 g^{-1} and most of the surface area was due to mesopores (0.184 cm^3 g^{-1}), where as only a low portion of surface area was due to micropores (0.022 cm^3 g^{-1}). SB pore volume was higher than many other biochars reported in Table 1 and in the literature (e.g. [11].

The cation exchange capacity (CEC) corresponds to the ability of the biomass to bind cations by an anion exchange mechanism and is equal to the number of negatively charged sites per unit of biomass mass [22]. The CEC value of studied straw biochar produced at 525 °C was 99.7 mmol/kg. Gai et al. [16] described the effect of pyrolysis temperature on CEC, reporting that wheat straw biochar produced at 400 and 500 °C had higher values of CEC than that at 600 and 700 °C. This is consistent with the findings of Lehmann et al. [32] that higher pyrolysis temperatures cause a decrease in the CEC, especially in charge density as a result of the greater surface area produced at high temperatures of up to 600 °C and loss of

Table 1 Physico-chemical properties of biochars pyrolyzed from *Triticum aestivum* and *Zea mays* biomass

	Wheat straw BC	Wheat straw BC	Corn straw BC	Corn straw BC	Wheat straw BC	Wheat straw BC	Wheat straw BC	Wheat straw BC
Pyrolysis temperature [°C]	525	400	600	450	500	750	700	500
Contact time [h]	2	2	2	4	4	2	4	1.5
pH	9.4	9.1	9.6	–	9.2	9.5	10.7	8.3
SA [m^2 g^{-1}] (BET)	66.79	4.8	13.08	44.97	2.48	467	319	111
CEC [μmol g^{-1}]	99.7[a]				201	–	15.4	51
Pore volume [cm^3 g^{-1}]	0.206	–	0.014	0.0345	–	0.26	–	0.09
Pore size [nm]	7.48	–	–	–	–	2.19	–	3.3
C [%]	74.4[a]	44.2	35.88	75.17	49.78	–	52.59	70.3
H [%]	2.83[a]	6.11	1.64	3.25	–	–	–	2.9
N [%]	1.04[a]	0.66	0.43	0.98	0.53	–	0.34	1.4
H/C	0.453	1.647	0.545	0.515	–	0.25	–	0.49
C/N	83.43	78.1	97.31	89.45	109.53	–	180.38	57.8
Literature	This study/[28][a]	[28]	[10]	[63]	[57]	[56]	[57]	[16]

[a] Data taken from Kloss et al. [28]

volatile matter, which may contain a substantial portion of the negative charge and the CEC as organic acids. However, when CEC values of different biochars are compared the method of determination and the biochar fraction used should be also taken into account. The above mentioned characteristics (pore volume, CEC, specific surface area) implied an excellent possibility for Cd^{2+} and Co^{2+} ions to be adsorbed by straw derived biochar.

Sorption equilibrium in single metal system

The separation processes of Cd^{2+} and Co^{2+} ions by straw-derived biochar were studied using a highly precise radiotracer method with the radionuclides ^{109}Cd and ^{60}Co. The adsorption equilibrium data were described by adsorption isotherms according to the Langmuir (Eq. 3; [31] and Freundlich (Eq. 4; [13] equations (Fig. 1). The isotherm parameters obtained from non-linear regression analyses are listed in Table 4. Coefficients of determination (R^2) related to the Langmuir model applied to Cd- and Co-sorption data were higher than those for the Freundlich model. Similarly, the sorption of Cd by water hyacinth biochars [11], garden green waste biochar, beech wood chips biochar [15], sesame straw biochar [41] and sorption of Co by *Chrysanthemum indicum* biochar [53] was best fitted by Langmuir isotherm.

The maximum sorption capacity Q_{max} of SB for Co^{2+} at pH 6.0 obtained from Langmuir isotherm was 89.7 ± 1.8 μmol g^{-1} and for Cd^{2+} ions 193 ± 10 μmol g^{-1}. The affinity constant b of the isotherms corresponds to the initial gradient, which indicates the biochar affinity at low concentrations of metal ions. A greater initial gradient corresponds to a higher affinity constant. From Fig. 1 it is evident that the cobalt isotherms are steeper at lower equilibrium concentrations than those for cadmium. In the case of b, cobalt sorption was recorded with 0.019 ± 0.003 dm^3 μmol^{-1} compared to 0.006 ± 0.001 dm^3 μmol^{-1} for cadmium. So straw derived biochar showed higher affinity towards cobalt, although the binding capacity in single element system was higher for cadmium. This was also reflected by higher Q_{max} value for Cd^{2+} (Table 2).

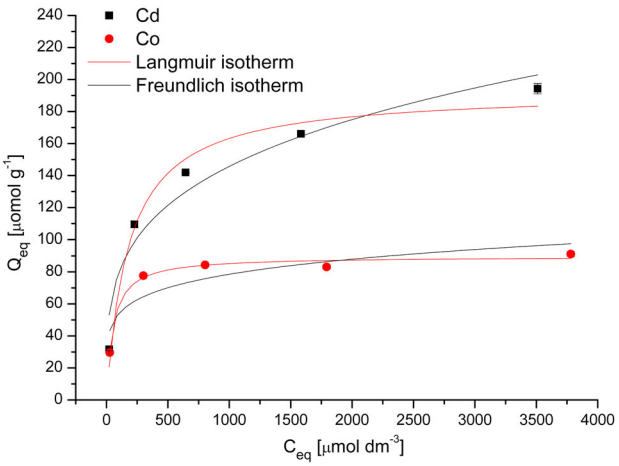

Fig. 1 Fit of the Langmuir and Freundlich isotherms of Cd^{2+} and Co^{2+} ions sorption by straw biochar (2.5 g dm^{-3}, d.w.) from single metal solutions after 4 h interaction at 22 °C and initial pH 6.0

The comparison of Q_{max} values determined from the Langmuir isotherm obtained in the present work with those of other authors indicates that sorption of Cd^{2+} ions by SB has been comparable with Cd sorption capacity of biochar prepared from different feedstock. However, in case of Co^{2+} ions sorption the Q_{max} value was distinctly lower in comparison with Q_{max} values from other studies (Table 3).

Cd and Co adsorption in binary system

Different toxic metals often occur simultaneously in contaminated environments. In comparison to single-metal adsorption, in binary and multicomponent mixtures metal ions in solution may interact or compete for the binding sites of the sorbent. For this reason, the influence of cadmium on cobalt sorption from a binary Co–Cd system has been investigated using the radionuclides ^{109}Cd and ^{60}Co. In such a case the radioindicator method offers a unique possibility to study competitive adsorption. Sorption of Co^{2+} and Cd^{2+} ions from binary systems at different initial molar ratios of Co:Cd is depicted in Fig. 2a, b. In comparison with single systems, the coexistence of Cd^{2+} and Co^{2+} ions influenced the sorption capacity of each other, advocating a competitive adsorption between Cd^{2+} and Co^{2+} ions. The sorption of cadmium was less affected by the presence of Co^{2+} ions than the cobalt sorption by the presence of Cd^{2+} ions in solution (Fig. 2a, b). The results indicated that at low Co and Cd concentrations in solution, binding of metal ions on different active sites of the SB surface occurred. At higher metal concentrations a significant decrease of Co sorption from 52 μmol g^{-1} (molar ratio Co:Cd—2:1) to 14.4 μmol g^{-1} (molar ratio Co:Cd—1:2) in the present of Cd was observed. Cd sorption by SB decreased in binary Cd-Co system from 162 μmol g^{-1} (molar ratio of Cd:Co—2:1) to 121 μmol g^{-1} (molar ratio of Cd:Co—1:2). When Co^{2+} and Cd^{2+} are present in equimolar ratio 1:1 maximum uptake was 34 μmol g^{-1} for Co and 162 μmol g^{-1} for Cd indicating significantly higher affinity of SB to Cd.

Building on the results from single metal experiments where Langmuir isotherm functions had shown a good fit to the experimental data of Co^{2+} and Cd^{2+} sorption reasonably well, the extended Langmuir model [4, 37] was used for quantitative interpretation of sorption equilibrium in Co-Cd binary systems.

Equations [4] and [5] were used to fit the experimental data and 3D sorption isotherm surfaces and corresponding parameters were obtained (Fig. 3, Table 4), where on the X and Y axis equilibrium concentrations C_{eqCo} and C_{eqCd} (μmol dm^{-3}) versus adsorbed amount Q_{eq} Co and Q_{eq} Cd (μmol g^{-1}) on the axis Z are plotted. Experimental values of Cd and Co uptake are shown as individual data points and the surfaces correspond to Cd or Co uptake as predicted by extended Langmuir model. High values of the coefficient of determination R^2 (0.883 for Co^{2+} and Cd^{2+} to 0.975) indicated that the extended Langmuir model described the experimental data of the binary system Co-Cd well. From 3D sorption surfaces it is evident that the sorption of Co^{2+} ions is strongly influenced by the presence of cadmium ions in solution (Fig. 3b) and during the adsorption process interactions and competitive mutual effects between ions occur.

Such interactions can be explained by the different affinity of Cd and Co ions towards binding sites on the SB surface. Significant differences between the values of affinity constants b_{Cd} and b_{Co} (Table 4) in the binary system Cd-Co confirmed higher affinity of SB to Cd ions in comparison with Co ions. Similarly, Park et al. [41] studied adsorption of Cr, Zn, Cd, Cu and Pb from multi-metal solutions by sesame straw biochar and found that the values of affinity constant b calculated from Langmuir isotherm decreased in the order: $b_{Cr} > b_{Zn} > b_{Cd} > b_{Cu} > b_{Pb}$. Adsorption sites of pruning-derived biochar were rather occupied by Pb and Cr and less by Cu in simultaneous metal sorption experiments [8]. This is consistent with the hypothesis that variance in affinity in multi-component systems could be attributed to different ionic characteristics of Cd^{2+} and Co^{2+} ions and physicochemical properties of SB. Some physico-chemical properties of cadmium and cobalt ions are presented in Table 5. The electronegativity constants of Cd^{2+} (1.69) and Co^{2+} (1.88) ions are not consistent with the obtained sorption capacities for metals (Table 6) indicating that surface electrostatic interactions did not play a significant role in sorption preferences in binary system. Similar results were postulated by Inyang et al. [24] in case of Cd, Ni and Cu sorption from mixtures by biochars derived from anaerobically digested biomass. However, Wang et al. [55] showed that adsorption of Ni^{2+} and Cd^{2+} ions by activated carbons produced by different activation methods was related to the nature of the metal ion (electronegativity and hydrated ionic radii) and the surface chemistry of carbons. According to the classification of metals based on covalent index [40], this reflects different ligand affinities as both cadmium and cobalt belong to borderline metal ions. The greater the covalent index value of metal ion is, the greater is the potential to form covalent bonds with ligands. At cation binding sites, borderline ions with higher $X_m^2 r$ displace borderline ions with lower $X_m^2 r$ which confirms our

Table 2 Langmuir and Freundlich equilibrium parameters (±SD) obtained by non-linear regression analysis for Co^{2+} and Cd^{2+} sorption by SB

Metal	Langmuir			Freundlich		
	Q_{max} (μmol g^{-1})	b (dm^3 μmol^{-1})	R^2	K (dm^3 g^{-1})	1/n	R^2
Co^{2+}	89.7 ± 1.8	0.019 ± 0.003	0.990	23.6 ± 7.9	0.26 ± 0.05	0.949
Cd^{2+}	193 ± 10	0.006 ± 0.001	0.977	25.4 ± 10.4	0.16 ± 0.06	0.802

Table 3 Comparison of maximum adsorption capacities of different biochar sorbents determined from Langmuir isotherm for Co^{2+} and Cd^{2+} ions

Biochar feedstock	pH	T (°C)	Pyrolysis temperature	Q_{max} Co^{2+} (μmol g^{-1})	Q_{max} Cd^{2+} (μmol g^{-1})	References
Miscanthus sacchariflorus	7.0	25	500	–	118	[27]
Beech wood chips	7.00	20	500	–	17.7	[15]
Garden green waste residues	7.00	20	500	–	69.4	[15]
Dairy manure	5.5	20	350	–	486	[60]
Rice straw biochar	5.0	25	400	–	302	[20]
Chrysanthemum indicum	5.0	30	650	771	–	[53]
Almond shell	7.0	20	650	477	–	[26]
Acacia nilotica leaf	5.0	–	300	602	–	[48]
Triticum aestivum	6.0	20	525	90	193	Present study

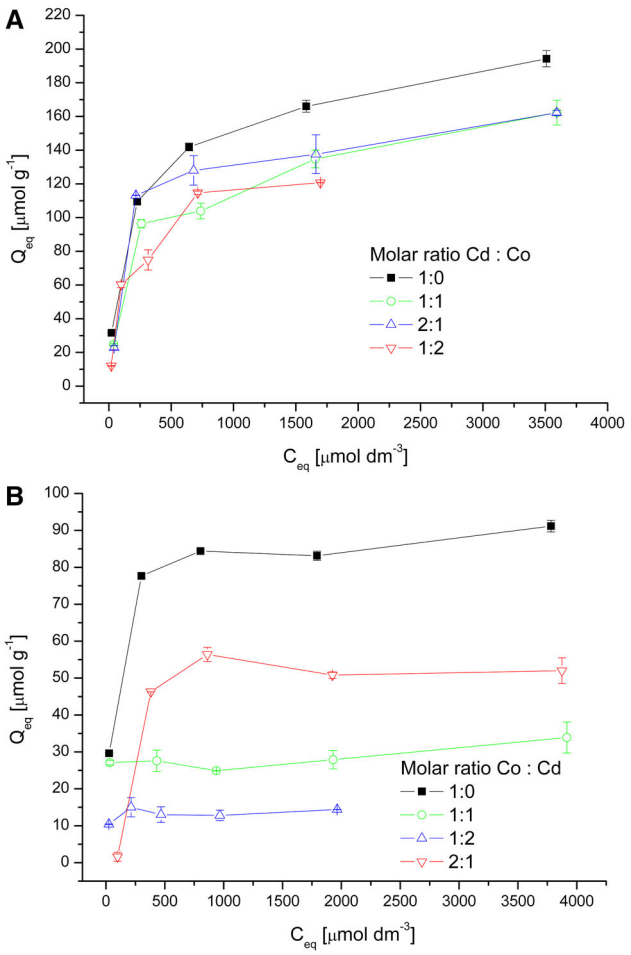

Fig. 2 Sorption of Cd^{2+} ions (**a**) and Co^{2+} ions (**b**) from binary Cd-Co system at different initial molar [Co]:[Cd] ratios by SB at pH 6.0 and 20 °C

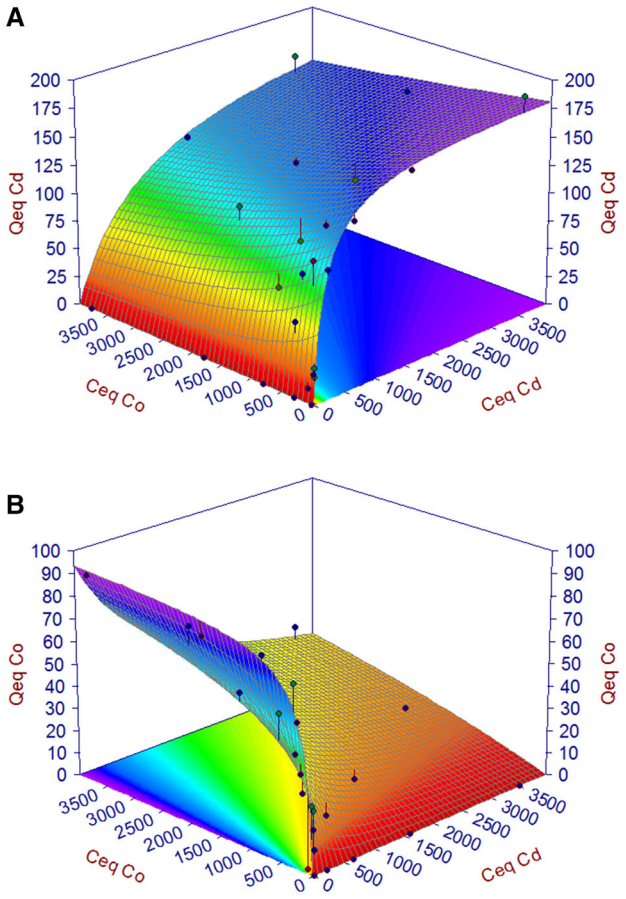

Fig. 3 3-D sorption isotherm surfaces of Cd-Co binary system: **a** Cd sorption (μmol g^{-1}); **b** Co sorption (μmol g^{-1}). The surfaces are predicted by the extended Langmuir model (Eqs. 4, 5) and the symbols are experimental data obtained at pH 6.0 and 20 °C

results from the binary system Cd^{2+}–Co^{2+}. It is reasonable to assume that higher affinity for Cd in binary system Cd–Co is also closely related to covalent index $\left(X_m^2 r\right)$ and ionic radius (Table 5). We pointed out that also solution chemistry (pH and metal speciation) significantly influenced the preference of SB for metals in binary system.

Table 4 Equilibrium parameters for Co^{2+} and Cd^{2+} sorption from binary mixtures Co-Cd by SB calculated from extended Langmuir model by non-linear regression analysis

Model	Q_{max} [μmol/g]	b_{Cd} [L/μmol]	b_{Co} [L/μmol]	R^2
$Q(Cd) = \frac{b_{Cd}Q_{maxCd}C_{eqCd}}{1+b_{Cd}C_{eqCd}+b_{Co}C_{eqCo}}$	189 ± 7	0.0055 ± 0.0008	0.0012 ± 0.0003	0.975
$Q(Co) = \frac{b_{Co}Q_{maxCo}C_{eqCo}}{1+b_{Co}C_{eqCo}+b_{Cd}C_{eqCd}}$	96 ± 7	0.0191 ± 0.0076	0.0073 ± 0.0029	0.902

Table 5 Some physico-chemical properties of cadmium and cobalt ions

Properties	Cd^{2+}	Co^{2+}
Atomic weight	112.41	58.93
Ionic radius r (pm)	97	72
Electronegativity (Pauling) X_m	1.69	1.88
Covalent index $\left(X_m^2 r\right)$	2.71	2.65

Mechanism of Cd and Co sorption by SB

Many papers dealing with metal sorption by biochar derived from various feedstocks discuss the metal uptake mainly on the basis of sorption kinetics, equilibrium isotherms, influence of temperature, pH and biochar dosage, although the mechanism of metal ion binding is not consistently studied. Appropriate analytical techniques are needed to elucidate the mechanisms participating in the sorption processes and to get insight into the localization and chemical nature of metals sorbed by various biochars. Therefore, in our work, the mechanistic aspects of Cd^{2+} and Co^{2+} sorption by SB were studied by different experimental approaches.

Influence of pH on Cd^{2+} and Co^{2+} sorption

The pH of the system is one of the most important environmental factors affecting sorption of toxic metals. The pH value strongly influences: (i) site dissociation of the biochar surface; (ii) solution chemistry (hydrolysis, complexation, redox reactions, precipitation, etc.); as well as (iii) ionization and speciation of metals in aqueous solutions. The influence of pH on the sorption of Co^{2+} and Cd^{2+} ions from single metal solutions onto straw derived biochar was determined in batch equilibrium experiments at pH values from 2.0 to 8.0 and the data are depicted in Figs. 4 and 5.

Co removal efficiency increased from 0.1 to 14 % with increasing solution pH from 2.0 to 4.0, remained stable till pH 6.0 and then increased further. Maximum Co removal efficiency (35 %) was observed at pH 8.0 (Fig. 4). Cd removal efficiency by SB (Fig. 5) increased with increasing pH and the maximum was reached at pH 8.0 (44 %). Slightly lower sorption was observed at pH 3.0 and minimum at pH 2.0 which could be closely related to the protonation of binding sites, resulting in a competition between H^+ and Co^{2+} or Cd^{2+} ions for sorption sites on the SB surface. The solution pH after sorption experiments increased from the initial values 2.0, 3.0, 4.0, 5.0, 6.0 and 8.0 to 2.2, 5.0, 6.7, 7.3, 7.6 and 9.0 due to the presence of alkaline components in straw biochar produced under the higher pyrolysis temperature [36]. As reported by Li et al. [33], the origin of biochar surface alkalinity receives less attention and is still under discussion, however, several contributions to alkalinity are proposed, e.g. oxygen-containing functional groups (pyrones, chromenes), oxygen-free sites (delocalized π electrons of the carbon basal plane), nitrogen-containing groups, and the constituents of the ash fraction of biochar.

Based on the speciation analysis of cobalt in a single sorption system (Fig. 4) predicted by the Visual MINTEQ speciation program at an initial concentration of 1000 μmol dm^{-3} of $CoCl_2$, cobalt at pH from 2.0 to 8.0 exists predominantly as Co^{2+} ion (99.9 %). Other ionic forms such as $CoOH^+$, $Co(OH)_2$, $Co(OH)^{3-}$ and $Co(OH)_4^{4+}$ are present in solution between pH 8.5 and 12.0 and precipitation of Co starts at pH > 8.5. Cadmium predominantly exists as Cd^{2+} (~88 %) and $CdCl^+$ (~10 %)

Table 6 The functional groups of straw derived biochar determined by FTIR analysis

Wave numbers (cm^{-1})	Vibration type
1740–1700	C = O stretching vibration of carboxyl, aldehyde, ketone, esters
1654	C = C stretching in the aromatic ring in the lignin
1476	C = C stretching, –C–H_2 bending (lignin carbohydrates) or carbonates (CO_3^{2-})
1200–1000	C–O stretching vibration (e.g. acetyl esters), P–O bond of phosphates
849	C–H bending or C–O out of plane deformation from carbonates (CO_3^{2-})

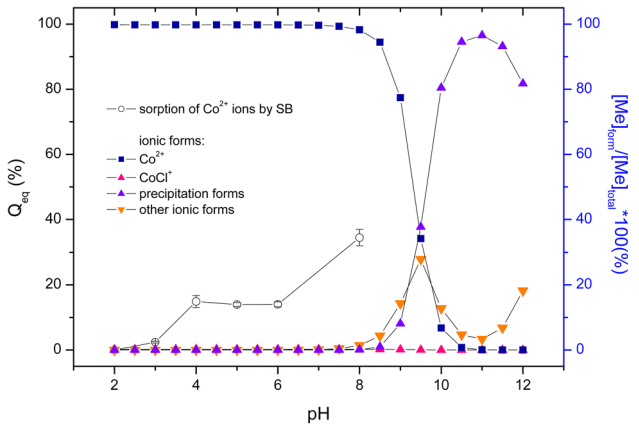

Fig. 4 Effect of initial pH on Q_{eq} sorption of Co (1000 μmol dm^{-3} $CoCl_2$, $^{60}CoCl_2$ 91 kBq dm^{-3}) by SB (2.5 g dm^{-3}, d.w.) from single metal solution and predicted Co speciation in solution. *Error bars* represent standard deviation (SD) of the mean ($n = 2$). Co speciation was calculated using Visual MINTEQ version 3.0 with initial conditions: 1000 μmol dm^{-3} $CoCl_2$, $T = 20$ °C, $pCO_2 = 38.5$ Pa

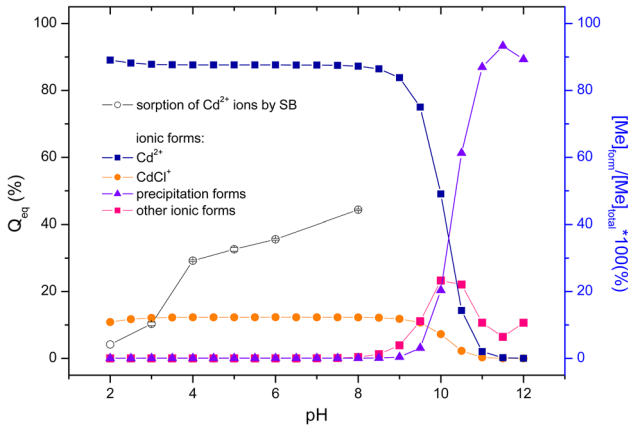

Fig. 5 Effect of initial pH on Q_{eq} sorption of Cd (1000 μmol dm^{-3} $CdCl_2$, $^{109}CdCl_2$ 49 kBq dm^{-3}) by SB (2.5 g dm^{-3}, d.w.) from single metal solution and predicted Cd speciation in solution. *Error bars* represent standard deviation (SD) of the mean ($n = 2$). Cd speciation was calculated using Visual MINTEQ version 3.0 with initial conditions: 1000 μmol dm^{-3} $CdCl_2$, $T = 20$ °C, $pCO_2 = 38.5$ Pa

cation forms within pH ranging from 2.0 to 7.5 (Fig. 5). A number of other ionic forms such as $CdOH^+$, Cd_2OH^{3+}, $Cd(OH)_3^-$ and $Cd(OH)_4^{2-}$ are present in solution between pH 8.0 and 12.0. The concentration of Cd^{2+} starts to decrease at pH > 8.0 and the precipitation of Cd started at pH > 9.0.

Markedly higher Co and Cd removal observed at pH 8.0 was related to precipitation (directly on SB surfaces or in solution), due to the increase of solution pH after the sorption and higher internal pH in the porous structure of SB. Moreover in the interpretation of Cd sorption onto SB it is necessary to consider the higher proportion of the monovalent cation $CdCl^+$ (~10 %). An increasing concentration of Cl^- in the environment will increase the proportion of $CdCl^+$ complexes [42]. Uchimiya [50] confirmed that Cd^{2+}sorption on biochar progressively increased as a function of pH and suggested that $CdOH^+$ and other hydrolysis products were the "reactive" Cd^{2+} species engaging in the surface interaction with biochar. Similarly, Kołodyńska et al. [30] achieved the maximum adsorption efficiency at a pH of about 5.0 for Cu^{2+} and Zn^{2+} and at pH 6.0 for Cd^{2+} and Pb^{2+}. Based on the obtained results, it is suggested that: [1] the binding of cadmium and cobalt ions was closely related to protonation of binding sites on the SB surface, resulting in competition between H^+ and H_3O^+ ions and Cd^{2+} and Co^{2+} ions for occupancy of the active sites; [2] cadmium and cobalt ions removal from solution also depended on metal speciation in solution and [3] the participation of cadmium and cobalt precipitation should not be neglected.

SEM and EDX elemental mapping

SEM/EDX analysis was carried out to observe the surface morphology of straw derived biochar before and after sorption of Co^{2+} and Cd^{2+} ions. The micrographs indicate that SB has an irregular amorphous surface with porous structure showing residual straw morphology (Fig. 6a). As reported by Liu et al. [35], this effect could be the result of a condensation and fusion process of the lignin and other small molecule compounds and inorganic compounds. A comparison of unloaded SB images and SB images after sorption exhibited no morphological changes on the biochar surfaces after sorption of Co^{2+} and Cd^{2+} ions (data not shown). Elemental mapping of SB after Cd and Co sorption illustrated spatial distribution of cobalt (Fig. 6c) and cadmium (Fig. 6b) on biochar surfaces. It can be seen that both metals effectively saturated specific areas on outer biochar surfaces. Moreno-Tovar et al. [39] using SEM-EDX elemental mapping confirmed uniform distribution of Cd on mesoporous activated carbon surfaces. We suppose that Co and Cd, after saturating the binding sites on the biochar's outer surfaces, are subsequently adsorbed to the network of pores and fissures that form the complex inner micro-structure of biochar. However, the spatial distribution of Co and Cd adsorbed on inner surfaces could not be visualized using EDX elemental mapping. Similar findings were observed by Beesley and Marmiroli [6] who studied immobilization and retention of soluble Cd and Zn by biochar.

FTIR spectroscopy

The straw derived biochar was characterized by FTIR analysis in the near IR region (4000–400 cm^{-1}) to identify major functional groups of straw derived biochar and their possible participation on sorption of Cd^{2+} and Co^{2+} ions.

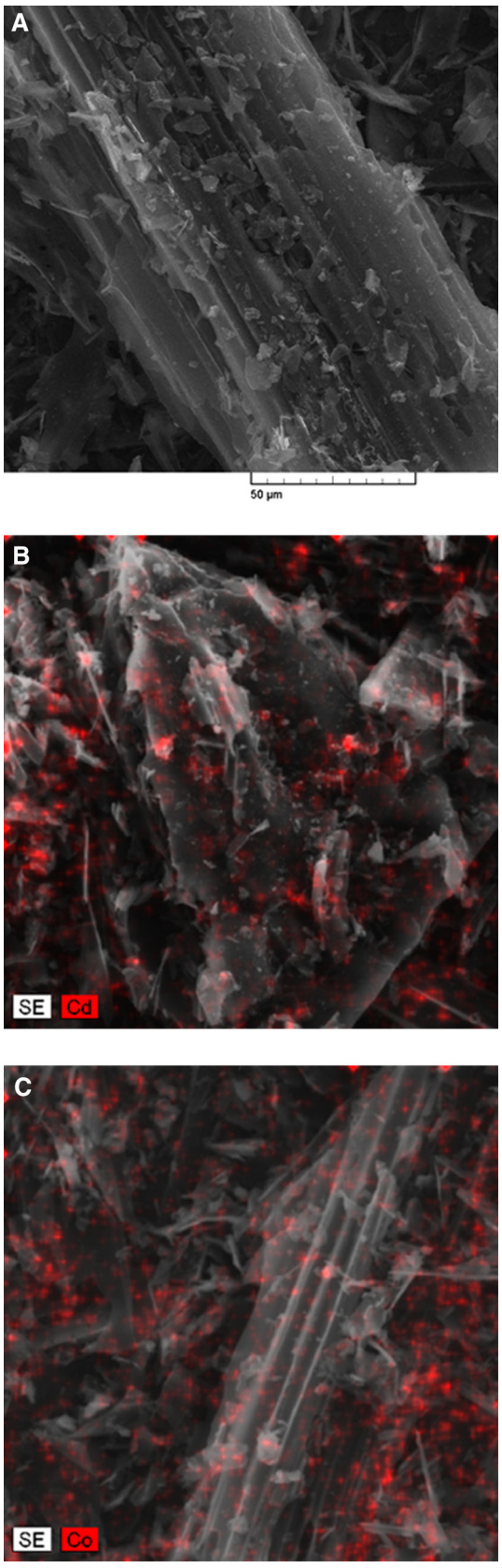

◀**Fig. 6** SEM-EDX analysis and elemental mapping of SB: **a** before and **b** after Co^{2+} (4000 µM $CoCl_2$) and **c** Cd^{2+} (4000 µM $CdCl_2$) sorption from single systems at pH 6.0

Table 6 presents band assignments of SB FTIR spectra before metal ions sorption. We pointed out that due to the number of probable functional groups, only those presented in high concentrations were identified. Pyrolysis of straw feedstock at 525 °C resulted in the evaporation of water, which led to the disappearance of the bands assigned to vibrations of OH groups at 3500–3200 cm^{-1} and aliphatic C-H stretching vibration due to the demethoxylation, demethylation and dehydration of lignin. As was reported by Kloss et al. [28] and Wang et al. [57] higher pyrolysis temperature presents an important factor, which affects the loss of OH and aliphatic groups as well as the increasing of pore formation and surface area of biochar. Higher pyrolysis temperature caused also the decrease of carboxylic and carbonylic functional groups and formation of aromatic and hydrophobic substances [56]. The band widths 1740–1700 cm^{-1} could be assigned to C = O vibrations of carboxyl, aldehyde, ketone and ester groups in lignocellulosic material. Careful examination revealed also several bands at 1654 cm^{-1} characteristic for C = C vibrations. As was observed by Melo et al. [38], bands at 1600 cm^{-1} represent aromatic systems in double bonds between carbons, but they may also be related to the double bonds between carbon and oxygen in amides. The bands at 1476 and 849 cm^{-1} are associated with vibrations of aromatic structures and may be also caused by carbonates (CO_3^{2-}) [28]. The peak around 1100 cm^{-1} could be assigned to C–O and C–O–C groups [56] or P–O bond of phosphates [52] indicating the presence of oxygen-containing groups on SB surfaces.

FTIR spectra (not shown) of SB showed that the peaks of carboxylic and carbonylic groups expected at 1740 cm^{-1} had shifted to higher wavenumbers after both Cd and Co sorption, confirming their role in metal binding. Although carboxylic and carbonylic groups contribute to negative a surface charge which is essential for metal cation retention, relatively low cation exchange capacity of SB (99.7 µmol g^{-1}, Table 1) indicated that ion exchange was not a predominant sorption mechanism. Precipitation would occur between Cd and Co and anions such as CO_3^{2-} or PO_4^{2-} released from the minerals in biochar which is consistent with the identification of CO_3^{2-} and P–O of phosphates on SB FTIR spectra and with results obtained by Zhang et al. [62]. By using XPS and XRD analyses, these authors confirmed that Cd precipitated as $CdCO_3$, Cd_3P_2 and $Cd_3(PO_4)_2$ on the surface of biochar derived from water hyacinth. The participation of other groups was supported by the changes of bands at 849, 1476 and

1654 cm^{-1}. Also Li et al. [33] have postulated that ion exchange and surface complexation play a negligible role in Cu^{2+} removal by *Spartina alterniflora* derived biochar. They expected that other mechanisms such as Cπ-cation interaction and precipitation might contribute to the Cu^{2+} removal by SABC. Data obtained by Harvey et al. [21] support Cd^{2+} sorption occurring predominantly on uncharged functional groups via cation-π bonding mechanisms. In case of low charge-highly carbonized biochars this mechanism most probably involved Cd^{2+} bonding with electron rich domains on graphene-like structures.

Based on the obtained results and literature review we stated that the main mechanisms of Cd and Co adsorption were related to charged and uncharged functional groups of straw derived biochar. But it is important to point out that in addition to functional groups biochar from straw feedstock has determinative mineralogical characteristics. Straw derived biochar used in our study contained sylvite (KCl), calcite ($CaCO_3$) and apatite (phosphate mineral) [28] and these minerals could serve as additional adsorption sites on biochar. This is in agreement with results obtained by Peld et al. [43] who studied sorption of Cd^{2+} and Zn^{2+} in apatite—aqueous system and found that apatite immobilize toxic metals with the sorption capacity up to 0.79 mmol g^{-1} for both Cd^{2+} and Zn^{2+}, respectively.

Conclusions

Data presented in our paper confirmed high adsorption capacity of SB for Cd and Co ions both in single and binary systems. Experimental equilibrium data of the single-component systems for Cd^{2+} and Co^{2+} ions have been well described by the Langmuir isotherm and the maximum sorption capacities, Q_{max}, were 193 ± 10 μmol g^{-1} for Cd^{2+} and 89.7 ± 1.8 μmol g^{-1} for Co^{2+} ions. In binary system, the presence of Cd^{2+} in different molar [Cd]:[Co] ratios caused significant decrease in Co^{2+} sorption indicating higher affinity of straw biochar toward Cd^{2+} ions. The main mechanisms of Cd and Co adsorption were related to charged and uncharged functional groups of straw derived biochar and metal ions precipitation. However, minerals (sylvite, calcite, apatite) present in SB could serve as additional adsorption sites. These results demonstrate that straw-based biochar is not only an effective nutrient vector for the benefit of soil fertility [29] but also a promising heavy metal-immobilizing agent for contaminated soils or water.

Acknowledgments This work was supported by a project of the Operational Program Research and Development and cofinanced by the European Regional Development Fund (ERDF) with the Grant Number ITMS 26220220191.

References

1. Adamcová R, Suraba V, Krajňák A, Rosskopfová O, Galamboš M (2014) First shrinkage parameters of Slovak bentonites considered for engineered barriers in the deep geological repository of high-level radioactive waste and spent nuclear fuel. J Radioanal Nucl Chem 302:737–743
2. Ahmad M, Lee SS, Dou X, Mohan D, Sung JK, Yang JE, Ok YS (2012) Effects of pyrolysis temperature on soybean stover- and peanut shell-derived biochar properties and TCE adsorption in water. Bioresour Technol 118:536–544
3. Ahmad M, Rajapaksha AU, Lim JE, Zhang M, Bolan N, Mohan D, Vithanage M, Lee SS, Ok YS (2014) Biochar as a sorbent for contaminant management in soil and water: a review. Chemosphere 99:19–33
4. Apiratikul R, Pavasant P (2006) Sorption isotherm model of binary component sorption of copper, cadmium, and lead ions using dried green macroalga, *Caulerpa lentillifera*. Chem Eng J 119:135–145
5. Barrett EP, Joyner LG, Halenda PP (1951) The determination of pore volume and area distributions in porous substances. I. Computations from nitrogen isotherms. J Am Chem Soc 73:373–380
6. Beesley L, Marmiroli M (2011) The immobilization and retention of soluble arsenic, cadmium and zinc by biochar. Environ Pollut 159:474–480
7. Cao XD, Harris W (2010) Properties of dairy-manure-derived biochar pertinent to its potential use in remediation. Bioresour Technol 101:5222–5228
8. Caporale AG, Pigna M, Sommella A, Conte P (2014) Effect of pruning-derived biochar on heavy metals removal and water dynamics. Biol Fert Soils 50:1211–1222
9. Chen B, Chen Z (2009) Sorption of naphthalene and 1-naphthol by biochars of orange peels with different pyrolytic temperatures. Chemosphere 76:127–133
10. Chen X, Chen G, Chen L, Chen Y, Lehmann J, McBride MB, Hay AG (2011) Adsorption of copper and zinc by biochars produced from pyrolysis of hardwood and corn straw in aqueous solution. Bioresour Technol 102:8877–8884
11. Ding Y, Liu Y, Liu S, Li Z, Tan X, Huang X, Zeng G, Zhou Z, Zheng B, Cai T (2016) Competitive removal of Cd(II) and Pb(II) by biochgars produced from water hyacinth: performance and mechanism. RSC Adv. doi:10.1039/C5RA26248H
12. Dong X, Wang CH, Li H, Wu M, Liao S, Zhang D, Pan B (2014) The sorption of heavy metals on thermally treated sediments with high organic matter content. Bioresour Technol 160:123–128
13. Freundlich HMF (1906) Über die adsorption in lösungen. Z Phys Chem 57:385–470
14 Frišták V, Pipíška M, Valovčiaková M, Lesný J, Rozložník M, (2014) Monitoring ^{60}Co activity for the characterization of the sorption process of Co^{2+} ions in municipal activated sludge. J Radioanal Nucl Chem 299:1607–1614
15. Frišták V, Pipíška M, Lesný J, Soja G, Friesl-Hanl W, Packová A (2015) Utilization of biochar sorbents for Cd2+, Zn2+ and Cu2+ ions separation from aqueous solutions: comparative study. Environ Monit Assess 187:4093
16. Gai X, Wang H, Liu J, Zhai L, Liu S, Ren T (2014) Effects of feedstock and pyrolysis temperature on biochar adsorption of ammonium and nitrate. PLoS One. doi:10.1371/journal.pone.0113888
17. Galamboš M, Suchánek P, Rosskopfová O (2012) Sorption of anthropogenic radionuclides on natural and synthetic inorganic sorbents. J Radioanal Nucl Chem 293:613–633
18. Gomes PC, Fontes MP, da Silva AG, de S Mendonca E, Netoo AR (2001) Selectivity sequence and competitive adsorption of heavy metals by Brazilian soils. Soil Sci Soc Am J 65:1115–1121

19. Gustafson J.P.: Visual-MINTEQ, version 3.0. (2010) http://www.lwr.kth.se/english/OurSoftware/Vminteq. Accessed May 2010
20. Han X, Liang CHF, Li TQ, Wang K, Huang HG, Yang X (2013) Simultaneous removal of cadmium and sulfamethoxazole from aqueous solution by rice straw biochar. J Zhejiang Univ Sci B 14:640–649
21. Harvey OR, Herbert BE, Rhue RD, Kuo LJ (2011) Metal interactions at the biochar-water interface: energetics and structure-sorption relationships elucidated by flow adsorption microcalorimetry. Environ Sci Technol 45:5550–5556
22. Hawari AH, Mulligan CN (2006) Heavy metals uptake mechanisms in a fixed-bed column by calcium-treated anaerobic biomass. Process Biochem 41:187–198
23. Horvath G, Kawazoe K (1983) Method for the calculation of effective pore-size distribution in molecular-sieve carbon. J Chem Eng Jpn 16:470–475
24. Inyang M, Gao B, Yao Y, Xue Y, Zimmerman AR, Pullammanappallil P, Cao X (2012) Removal of heavy metals from aqueous solution by biochars derived from anaerobically digested biomass. Bioresour Technol 110:50–56
25. Keiluweit M, Nico PS, Johnson MG, Kleber M (2010) Dynamic molecular structure of plant biomass-derived black carbon (biochar). Environ Sci Technol 44:1247–1253
26. Kılıc M, Kırbıyık C, Cepeliogullar Ö, Pütüna AE (2013) Adsorption of heavy metal ions from aqueous solutions by biochar, a by-product of pyrolysis. Appl Surf Sci 283:856–862
27. Kim WK, Shim T, Kim YS, Hyun S, Ryu Ch, Park YK, Jung J (2013) Characterization of cadmium removal from aqueous solution by biochar produced from a giant *Miscanthus* at different pyrolytic temperatures. Bioresour Technol 138:266–270
28. Kloss S, Zehetner F, Dellantonio A, Hamid R, Ottner F, Liedtke V, Schwanninger M, Gerzabek MH, Soja G (2012) Characterization of slow pyrolysis biochars: effect of feedstocks and pyrolysis temperature on biochar properties. J Environ Qual 41:990–1000
29. Kloss S, Zehetner F, Wimmer B, Bücker J, Rempt F, Soja G (2014) Biochar application to temperate soils: effects on soil fertility and crop growth under greenhouse conditions. J Plant Nutr Soil Sci 177:3–15
30. Kołodyńska D, Wnętrzak R, Leahy JJ, Hayes MHB, Kwapiński W, Hubicki Z (2012) Kinetic and adsorptive characterization of biochar in metal ions removal. Chem Eng J 197:295–302
31. Langmuir I (1918) Adsorption of gases on plane surfaces of glass, mica and platinum. J Am Chem Soc 40:1361–1403
32. Lehmann J, Rillig MC, Thies J, Masiello CA, Hockaday WC, Crowley D (2011) Biochar effects on soil biota—a review. Soil Biol Biochem 43:1812–1836
33. Li M, Liu Q, Guo L, Zhang Y, Lou Z, Wang Y, Qian G (2013) Cu(II) removal from aqueous solution by *Spartina alterniflora* derived biochar. Bioresource Technol 141:83–88
34. Liu Q, Wang S, Zheng Y, Luo Z, Cen K (2008) Mechanism study of wood lignin pyrolysis by usingm TG-FTIR analysis. J Anal Appl Pyrolysis 82:170–177
35. Liu Z, Zhang FS, Wu J (2010) Characterization and application of chars produced from pinewood pyrolysis and hydrothermal treatment. Fuel 89:510–514
36. Lu H, Zhang W, Yang Y, Huang X, Wang S, Qiu R (2012) Relative distribution of Pb^{2+} sorption mechanisms by sludge-derived biochar. Water Res 46:854–862
37. Markham EC, Benton AF (1931) The adsorption of gas mixtures by silica. J Am Chem Soc 53:497–507
38. Melo LCA, Coscione AR, Abreu CA, Puga AP, Camargo OA (2013) Influence of pyrolysis temperature on cadmium and zinc sorption capacity of sugar cane straw-derived biochar. BioResources 8:4992–5004
39. Moreno-Tovar R, Terrés E, Rangel-Mendez JR (2014) Oxidation and EDX elemental mapping characterization of an ordered mesoporous carbon: Pb(II) and Cd(II) removal. Appl Surf Sci 303:373–380
40. Nieboer E, Richardson HS (1980) The replacement of the non-descript term 'heavy metals' by a biologically and chemically significant classification of metal ions. Environ Pollut 3:3–26
41. Park JH, Ok YS, Kim SH, Cho JS, Heo JS, Delaune RD, Seo DC (2016) Competitive adsorption of heavy metals onto sesame straw biochar in aqueous solutions. Chemosphere 142:77–83
42. Partelová D, Šuňovská A, Marešová J, Horník M, Pipíška M, Hostin S (2015) Removal of contaminants from aqueous solutions using hop (*Humulus lupulus* L.) agricultural by-products. Nova Biotechnol Chim 14:212–227
43. Peld M, Tõnsuaadu K, Bender V (2004) Sorption and desorption of Cd^{2+} and Zn^{2+} ions in apatite-aqueous systems. Environ Sci Technol 38:5626–5632
44. Popova NN, Bykov GL, Petukhova GA, Pavlov YuS, Tananaev IG, Ershov BG (2013) Studies of physicochemical properties of modified carbon nanomaterials for sorption extraction of radionuclides. III. The effect of oxidizing treatment on sorption of Am(III) from aqueous solutions. Prot Met Phys Chem 49:304–308
45. Remenárová L, Pipíška M, Horník M, Rozložník M, Augustín J, Lesný J (2012) Biosorption of cadmium and zinc by activated sludge from single and binary solutions: mechanism, equilibrium and experimental design study. J Taiwan Inst Chem Eng 43:433–443
46. Shaheen SM, Derbalah AS, Moghanm FS (2012) Removal of heavy metals from aqueous solution by zeolite in competitive sorption system. Int J Environ Sci Dev 3:362–367
47. Shen Z, Jin F, Wang F, McMillan O, Al-Tabbaa A (2015) Sorption of lead by Salisbury biochar produced from British broadleaf hardwood. Bioresour Technol 193:553–556
48. Thilagavathy P, Santhi T (2014) Kinetics, isotherms and equilibrium study of Co(II) adsorption from single and binary aqueous solutions by acacia nilotica leaf carbon. Chin J Chem Eng 22:1193–1198
49. Trakal L, Šigut R, Šillerová H, Faturíková D, Komárek M (2014) Copper removal from aqueous solution using biochar: effect of chemical activation. Arab J Chem 7:43–52
50. Uchimiya M (2014) Influence of pH, ionic strength, and multidentate ligand on the interaction of CdII with biochars. ACS Sustain Chem Eng 2:2019–2027
51. Uchimiya M, Chang S, Klasson KT (2011) Screening biochars for heavy metal retention in soil: role of oxygen functional groups. J Hazard Mater 190:432–441
52. Uchimiya M, Lima IM, Thomas Klasson K, Chang S, Wartelle LH, Rodgers JE (2010) Immobilization of heavy metal ions (CuII, CdII, NiII, and PbII) by broiler litter-derived biochars in water and soil. J Agric Food Chem 58:5538–5544
53. Vilvanathan S, Shanthakumar S (2015) Biosorption of Co(II) ions from aqueous solution using Chrysanthemum indicum: kinetics, equilibrium and thermodynamics. Process Saf Environ Prot 96:98–110
54. Voronina AV, Blinova MO, Kulyaeva IO, Sanin PY, Semenishchev VS, Afonin YD (2015) Sorption of cesium radionuclides from aqueous solutions onto natural and modified aluminosilicates. Radiochemistry 57:522–529
55. Wang J, Liu H, Yang S, Zhang J, Zhang C, Wu H (2014) Physicochemical characteristics and sorption capacities of heavy metal ions of activated carbons derived by activation with different alkyl phosphate triesters. Appl Surf Sci 316:443–450
56. Wang P, Yin Y, Guo Y, Wang C (2015) Removal of chlorpyrifos from waste water by wheat straw-derived biochar synthesized through oxygen-limited method. RSC Adv 5:72572–72578

57. Wang Y, Hu Y, Zhao X, Wang S, Xing G (2013) Comparisons of biochar properties from wood material and crop residues at different temperatures and residence times. Energ Fuel 27:5890–5899
58. Wu W, Yang M, Feng Q, McGrouther K, Wang H, Lu H, Chen Y (2012) Chemical characterization of rice straw-derived biochar for soil amendment. Biomass Bioenerg 47:268–276
59. Wu Y, Fan Y, Zhang M, Ming Z, Yang S, Arkin A, Fang P (2016) Functionalized agricultural biomass as a low-cost adsorbent: utilization of rice straw incorporated with amine groups for the adsorption of Cr(VI) and Ni(II) from single and binary systems. Biochem Eng J 105:27–35
60. Xu X, Cao X, Zhao L, Wang H, Yu H, Gao B (2013) Removal of Cu, Zn, and Cd from aqueous solutions by the dairy manure-derived biochar. Environ Sci Pollut R 20:358–368
61. Yakkala K, Yu MR, Roh H, Yang JK, Chang YY (2013) Buffalo weed (*Ambrosia trifida* L. var. *trifida*) biochar for cadmium(II) and lead(II) adsorption in single and mixed system. Desalin Water Treat 51:7732–7745
62. Zhang F, Wang X, Yin D, Peng B, Tan C, Liu Y, Tan X, Wu S (2015) Efficiency and mechanisms of Cd removal from aqueous solution by biochar derived from water hyacinth (*Eichornia crassipes*). J Environ Manage 153:68–73
63. Zhao X, Ouyang W, Hao F, Lin Ch, Wang F, Han S, Geng X (2013) Properties comparison of biochars from corn straw with different pretreatment and sorption behavior of atrazine. Bioresour Technol 147:338–344